Preprint of:
S. Bayoudh, T. A. Nieminen, N. R. Heckenberg and H. Rubinsztein-Dunlop
"Orientation of biological cells using plane-polarized Gaussian beam optical tweezers"
Journal of Modern Optics **50**(10), 1581–1590 (2003)
Changes: Corrections to equations (6) and (7).

Orientation of biological cells using plane-polarized Gaussian beam optical tweezers

S. Bayoudh, T. A. Nieminen, N. R. Heckenberg and H. Rubinsztein-Dunlop

Centre for Biophotonics and Laser Science, Department of Physics
The University of Queensland, Brisbane, QLD 4072, Australia.
tel: +61-7-3365 3405, fax: +61-7-3365 1242,
e-mail: timo@physics.uq.edu.au

Abstract

Optical tweezers are widely used for the manipulation of cells and their internal structures. However, the degree of manipulation possible is limited by poor control over the orientation of trapped cells. We show that it is possible to controllably align or rotate disc shaped cells—chloroplasts of *Spinacia oleracea*—in a plane polarised Gaussian beam trap, using optical torques resulting predominantly from circular polarisation induced in the transmitted beam by the non-spherical shape of the cells.

1 Introduction

Optical tweezers are widely used for the manipulation of cells and their internal structures [1]. A strongly focussed laser beam is used to apply piconewton forces, which is sufficient to trap or to move cells in three dimensions. However, there is poor control of the orientation of cells within the trap. While a variety of methods to rotate microscopic objects have been demonstrated, they are either dependent on absorption [2, 3], making them unsuitable for biological applications, restricted to special types of particles [4, 5, 6], or make use of multiple beams or special types of beams [7, 8, 9]. The latter methods can, in principle, be used for the rotation of biological specimens, but either add a great deal of complexity to the required apparatus, or use expanded non-symmetric focal spots, reducing the possibility of three-dimensional trapping.

The alignment of elongated dielectric particles within static fields suggests that it might be possible to align non-spherical trapped objects simply by using a plane polarised trapping beam. Unlike rod shaped objects, which tend to align along the beam axis [10] leaving no remaining asymmetry with respect to the plane of polarisation, disc shaped objects, aligned with the beam axis, retain an asymmetric shape perpendicular to the beam axis and should also align with the plane of polarisation. Such an alignment scheme has the dual advantages of being easy to implement using an existing optical tweezers apparatus, and providing maximum trapping efficiency. The torques acting to align a dielectric object within a static field result from the induced polarisation within the object being at an angle to the applied field. It would, however, be questionable to naïvely apply the static field results to trapping by optical fields.

We demonstrate experimentally that sufficient torque is generated for the technique to be useful for biological specimens—chloroplasts of *Spinacia oleracea* in our experiments—and calculate the optical force and torque using a full electromagnetic wave solution of Maxwell's equation to show unambiguously that the torque can be accounted for by the non-spherical shape of the chloroplasts.

2 Observation of alignment of chloroplasts

A standard optical tweezers setup using an inverted microscope was used. The only modification required for the alignment experiments was the addition of a half-wave plate on a rotatable mount to control the direction of the plane of polarisation (see figure 1). A Nd–YAG laser at 1064 nm was used, focussed by a 100× oil-immersion object of numerical aperture 1.3 to produce the trap.

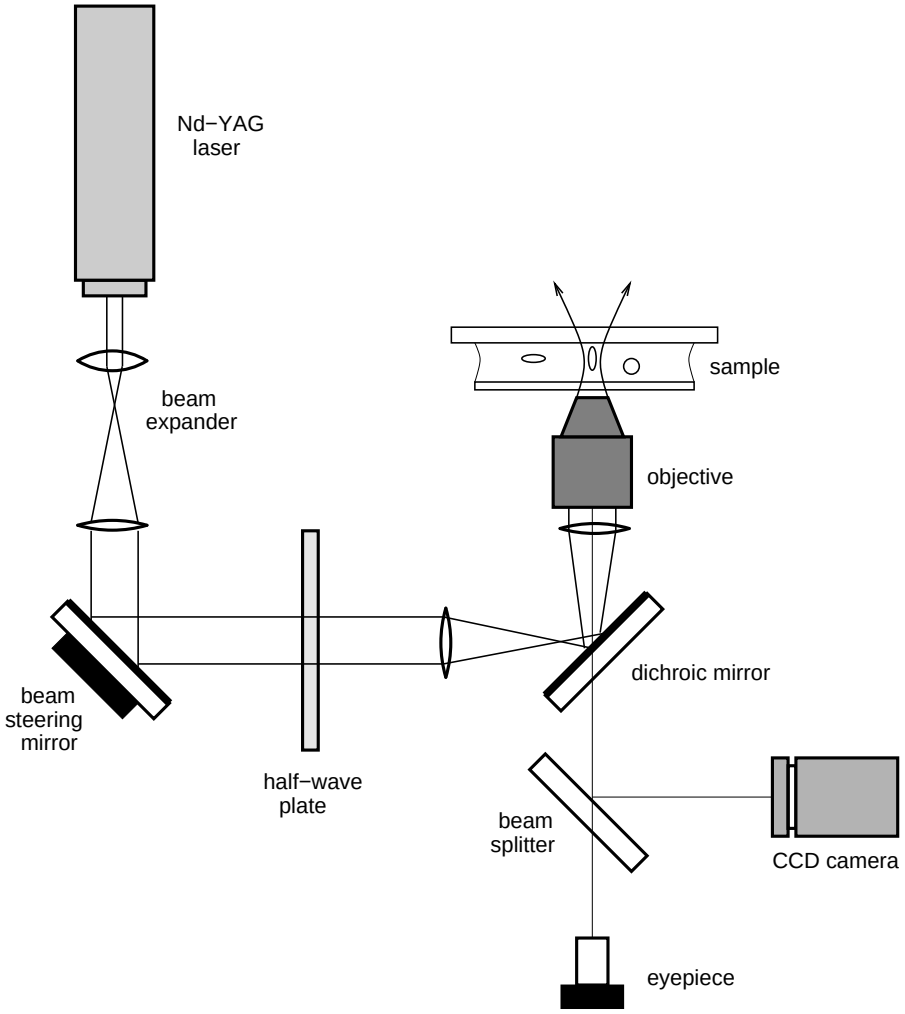

Figure 1: Schematic diagram of optical tweezers system for alignment of biological cells. The apparatus is a conventional optical tweezers setup with the addition of a half-wave plate in a rotatable mounting, allowing the plane of polarisation of the initially plane polarised trapping beam to be rotated.

Chloroplasts were isolated from fresh spinach leaves (*Spinacia oleracea* L.) using a buffer solution containing 0.4 M sucrose, 0.05 M HEPES, 0.01 M KCl, 0.0001 M $MgCl_2$ with a pH of 7.8. Chloroplasts were three-dimensionally trapped in the buffer solution using a beam power of 30 mW at the specimen plane. Trapped chloroplasts were observed to align with the plane of polarisation of the trapping beam. As the plane of polarisation of the trapping beam was rotated, the chloroplasts rotated so as to re-align with the beam, taking on the order of a second or two to do so. Alignment of a chloroplast is shown in figure 2.

Since the observed alignment is similar to that expected from birefringent particles [5], it necessary to exclude this possibility. This was done by replacing the half-wave plate with a quarter wave plate to produce a circularly polarised trapping beam. If the chloroplasts were sufficiently birefringent so as to align with the plane polarised beam, the circularly polarised beam should have caused them to rotate at a constant rate [5]. Chloroplasts were not observed to rotate or align in the circularly polarised beam. No birefringence could be detected when viewing chloroplasts between crossed

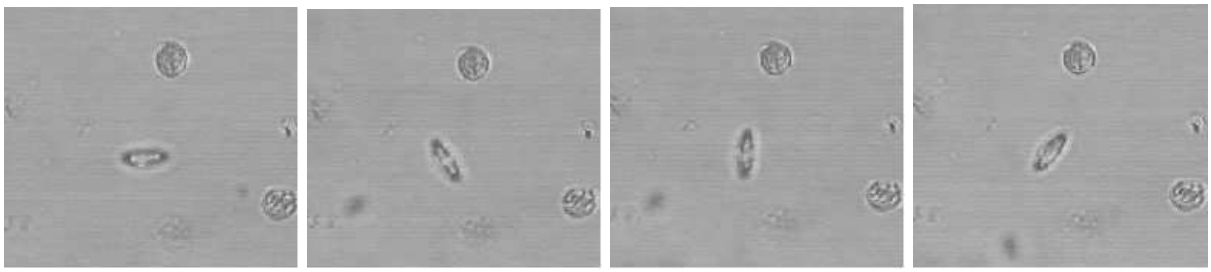

Figure 2: Alignment of chloroplasts with the plane of polarisation of the trapping beam. The frames show rotation of a chloroplast as the plane of polarisation of the trapping beam is rotated. In each frame, the chloroplast lies in the plane of polarisation. The chloroplast is approximately 4 μm long along the long axis.

polarisers.

3 Optical force and torque

Optical forces and torque are a necessary result of the conservation of momentum and angular momentum when a particle scatters light, changing the momentum or angular momentum. Therefore, if the scattering of the trapping beam by the trapped cell can be calculated, the optical force and torque can be calculated [11].

The chloroplasts that we wish to model scattering by are too large for the Rayleigh (ie small particle) approximation to be valid, and too thin for the geometric optics approximation to be valid. Therefore, a full EM wave scattering calculation is needed. We calculate the scattered fields using the T-matrix method [12, 13, 14, 15], in which, as in generalised Lorenz-Mie theory (GLMT) [16], the incident and scattered fields are expanded in terms of vector spherical wavefunctions (VSWFs), which are the electric and magnetic multipole fields. Unlike GLMT, the T-matrix method does not require the surface of the particle to be a constant surface in a separable coordinate system.

Apart from being computationally well-suited for optical tweezers calculations since the T-matrix for a given particle needs to be calculated only once [11, 15], the mathematical formulation of the T-matrix method is physically enlightening since the VSWFs are simultaneous eigenfunctions of the total angular momentum operator, with eigenvalues $[n(n+1)]^{1/2}$, and the z-component of angular momentum operator, with eigenvalues m.

In our T-matrix calculations, the incoming and outgoing fields are expanded in terms of incoming and outgoing VSWFs:

$$\mathbf{E}_{\mathrm{inc}}(\mathrm{r}) = \sum_{n=1}^{\infty}\sum_{m=-n}^{n} a_{nm}\mathbf{M}_{nm}^{(2)}(k\mathrm{r}) + b_{nm}\mathbf{N}_{nm}^{(2)}(k\mathrm{r}). \quad (1)$$

$$\mathbf{E}_{\mathrm{scat}}(\mathrm{r}) = \sum_{n=1}^{\infty}\sum_{m=-n}^{n} p_{nm}\mathbf{M}_{nm}^{(1)}(k\mathrm{r}) + q_{nm}\mathbf{N}_{nm}^{(1)}(k\mathrm{r}). \quad (2)$$

where the VSWFs are

$$\mathbf{M}_{nm}^{(1,2)}(k\mathrm{r}) = N_n h_n^{(1,2)}(kr)\mathbf{C}_{nm}(\theta,\phi) \quad (3)$$

$$\mathbf{N}_{nm}^{(1,2)}(k\mathrm{r}) = \frac{h_n^{(1,2)}(kr)}{krN_n}\mathbf{P}_{nm}(\theta,\phi) + N_n\left(h_{n-1}^{(1,2)}(kr) - \frac{nh_n^{(1,2)}(kr)}{kr}\right)\mathbf{B}_{nm}(\theta,\phi) \quad (4)$$

where $h_n^{(1,2)}(kr)$ are spherical Hankel functions of the first and second kind, $N_n = [n(n+1)]^{-1/2}$ are normalisation constants, and $\mathbf{B}_{nm}(\theta,\phi) = \mathbf{r}\nabla Y_n^m(\theta,\phi)$, $\mathbf{C}_{nm}(\theta,\phi) = \nabla\times(\mathbf{r}Y_n^m(\theta,\phi))$, and

$\mathbf{P}_{nm}(\theta,\phi) = \hat{\mathbf{r}}Y_n^m(\theta,\phi)$ are the vector spherical harmonics [12, 13, 14, 17], and $Y_n^m(\theta,\phi)$ are normalised scalar spherical harmonics. The usual polar spherical coordinates are used, where θ is the co-latitude measured from the $+z$ axis, and ϕ is the azimuth, measured from the $+x$ axis towards the $+y$ axis. It should be noted that our division of the fields into a purely incoming incident field and an outgoing scattered field is unusual; it is much more common to include the outgoing field resulting from the incident field in the absence of a scatterer as part of the incident field. Both formulations are equivalent [18]; our choice simplifies the expressions for optical force and torque. In practice, the field expansions and the T-matrix must be terminated at some finite $n = N_{\max}$ chosen so that the numerical results converge with sufficient accuracy [18, 19].

The normalised torque about the z-axis acting on the trapped particle is

$$\tau_z = \sum_{n=1}^{\infty}\sum_{m=-n}^{n} m(|a_{nm}|^2 + |b_{nm}|^2 - |p_{nm}|^2 - |q_{nm}|^2)/P \tag{5}$$

in units of $\hbar$ per photon, where $P = \sum_{n=1}^{\infty}\sum_{m=-n}^{n} |a_{nm}|^2 + |b_{nm}|^2$ is proportional to the incident power (omitting a unit conversion factor which will depend on whether SI, Gaussian, or other units are used). This torque includes contributions from both spin and orbital components; the spin torque about the z-axis is given by [20]

$$\begin{aligned}\sigma_z &= \frac{1}{P}\sum_{n=1}^{\infty}\sum_{m=-n}^{n}\frac{m}{n(n+1)}(|a_{nm}|^2 + |b_{nm}|^2 - |p_{nm}|^2 - |q_{nm}|^2)\\ &\quad -\frac{2}{n+1}\left[\frac{n(n+2)(n-m+1)(n+m+1)}{(2n+1)(2n+3)}\right]^{\frac{1}{2}}\\ &\quad \times\mathrm{Im}(a_{nm}b^{\star}_{n+1,m} + b_{nm}a^{\star}_{n+1,m} - p_{nm}q^{\star}_{n+1,m} - q_{nm}p^{\star}_{n+1,m}).\end{aligned} \tag{6}$$

The remainder of the torque is the orbital contribution. The axial trapping efficiency Q is [20]

$$\begin{aligned}Q &= \frac{2}{P}\sum_{n=1}^{\infty}\sum_{m=-n}^{n}\frac{m}{n(n+1)}\mathrm{Re}(a^{\star}_{nm}b_{nm} - p^{\star}_{nm}q_{nm})\\ &\quad -\frac{1}{n+1}\left[\frac{n(n+2)(n-m+1)(n+m+1)}{(2n+1)(2n+3)}\right]^{\frac{1}{2}}\\ &\quad \times\mathrm{Im}(a_{nm}a^{\star}_{n+1,m} + b_{nm}b^{\star}_{n+1,m} - p_{nm}p^{\star}_{n+1,m} - q_{nm}q^{\star}_{n+1,m}).\end{aligned} \tag{7}$$

The expansion coefficients of the outgoing (ie scattered) field are found from the expansion coefficients of the incoming field using the T-matrix:

$$\mathbf{p} = \mathbf{T}\mathbf{a}. \tag{8}$$

where $\mathbf{a}$ and $\mathbf{p}$ are vectors formed from the expansion coefficients of the incident wave (a_{nm} and b_{nm}) and the scattered wave (p_{nm} and q_{nm}). The expansion coefficients of the incoming field are calculated using far-field point-matching [19], and the T-matrix is calculated using a row-by-row point-matching method, exploiting symmetry of the particle when possible [18].

4 Optical force and torque on trapped chloroplasts

We model chloroplasts as oblate spheroids. Our numerical results are calculated for a spheroid of aspect ratio 4, with semi-minor axis of 0.5 μm and semi-major axes 2.0 μm. This is typical of the size and aspect ratio of the chloroplasts aligned in our experiment. In reality, one face of the chloroplasts is concave [21], but our simplified geometry serves as a general model for disc shaped cells and organelles, and adequately models the almost disc shaped chloroplasts. At the trapping wavelength of 1064 nm, the refractive index of the chloroplast is assumed to be 1.4, which is typical of organelles such as mitochondria and nuclei as well as chloroplasts. Therefore, the results for chloroplasts,

including both experimental observations and theoretical caclulations, are also applicable to other organelles of similar size and shape. The refractive index of the sucrose solution in which the chloroplasts are trapped is 1.35. The trapping beam was chosen to reproduce the focal spot size in the trap. The focal spot is elliptical, with radii of 0.60 μm and 0.54 μm along and perpendicular to the plane of polarisation, respectively. The ellipticity of the beam spot is a consequence of strongly focussing a plane polarised vector beam [19, 24].

The axial trapping efficiency is shown in figure 3. The equilibrium position of the chloroplast in the observed orientation (aligned with the plane of polarisation) is with its centre 1.20 μm beyond the beam focus. Since the chloroplasts are three-dimensionally trapped during the course of the experiment, torques are evaluated when the chloroplast is at this equilibrium position within the trap.

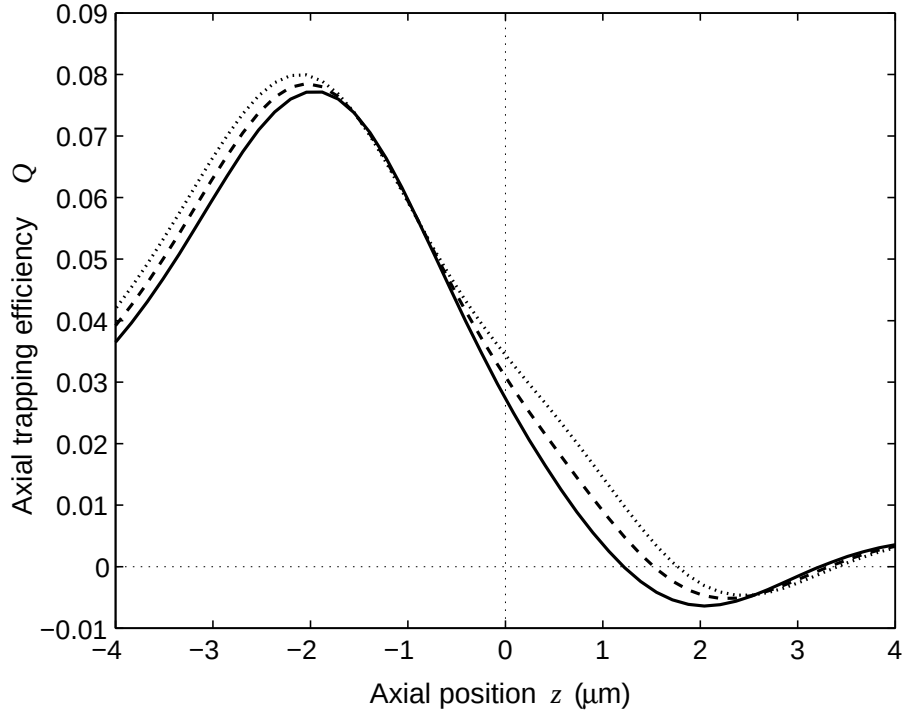

Figure 3: Axial trapping efficiency. The trapping efficiency is shown for an oblate spheroidal chloroplast with semi-minor axis 0.5 μm and semi-major axes 2 μm. The trapping efficiency is shown for chloroplasts aligned along the beam axis, at varying angles to the plane of polarisation. The force is shown for chloroplasts aligned with the plane of polarisation (solid line), at 45° to (dashed line), and perpendicular to the plane of polarisation (dotted line). The equilibrium position in all cases is with the centre of the chloroplast slightly beyond the focal plane of the beam located at $z = 0$.

The torques acting to align the plane of the chloroplast with the beam axis and the plane of polarisation are shown in figure 4. The torque acting to align the chloroplast with the beam axis depends on the axis about which the chloroplast rotates. However, this torque is always much larger than the torque aligning the chloroplast with the plane of polarisation. Noting that the drag torque acting on the chloroplast will be on the order of the drag torque that would act on a sphere of radius equal to the semi-major axis of the chloroplast, we can estimate that the drag torque will be of order $\tau_{\text{drag}} = 8\pi\mu a^3\Omega = D\Omega$ where μ is the dynamic viscosity of the medium ($\approx 10^{-3}\,\text{Nsm}^{-2}$ for water, and $\approx 1.48 \times 10^{-3}\,\text{Nsm}^{-2}$ for the sucrose solution in our experiments), a is the semi-major axis of the chloroplast, and Ω is the rotation rate of the chloroplast. For the chloroplast considered here, the drag coefficient $D \approx 0.3\,\text{pN}\mu\text{ms/rad}$. For the beam power used in our experiments, 30 mW, the mean torque acting to align the chloroplast with the beam axis is about 3.8 pNμm, giving a mean rotation speed of $\approx 13\,\text{rad/s}$, so the chloroplasts can be expected to take on the order of a tenth of a second, or less depending on the initial position, to align with the beam axis. The torque acting to align the chloroplast with the plane of polarisation is much smaller, with a mean value of 0.22 pNμm, giving

a mean rotation speed of $\approx 0.73\,\mathrm{rad/s}$, and an alignment time on the order of 2 s. This is consistent with observations made during the experiment.

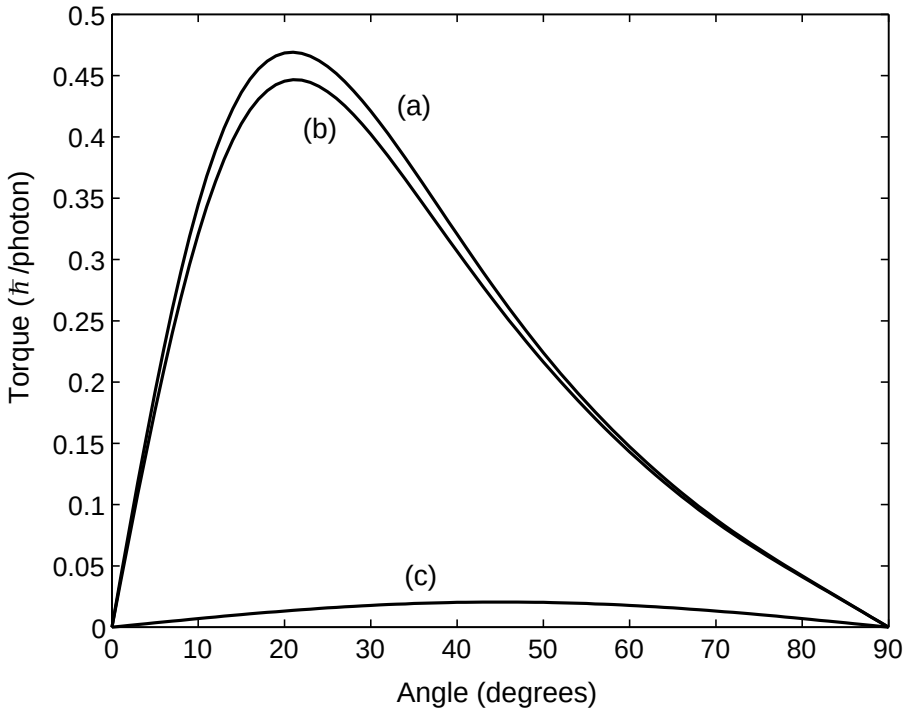

Figure 4: Alignment torque on chloroplasts. The torque is shown for alignment with the beam axis with the axis of rotation (a) perpendicular to the plane of polarisation and (b) parallel to the plane of polarisation, and (c) for alignment with the plane of polarisation by rotation about the beam axis after the chloroplast has aligned with the beam axis. The angle is the angle between the plane of the chloroplast and the beam axis/plane of polarisation.

The numerical results agree well with the observed behaviour of the chloroplasts, allowing us to unambiguously identify the non-spherical shape of the chloroplasts as the cause of their alignment with the plane of polarisation of the beam. The spin and orbital contributions to the alignment torque are shown in figure 5. The spin torque is approximately 23 times larger than the orbital torque, for all angles between the plane of the chloroplast and the plane of polarisation for which the torque is non-zero. Therefore, the torque is predominantly due to circular polarisation of the transmitted light resulting from scattering by the chloroplast.

The polarisation of the transmitted light is affected by the scattering process due to the differing dielectric polarisability of the chloroplast parallel to its long and short axes [22]. This results in a phase difference between the plane-polarised components in the transmitted beam parallel to the long and short axes of the chloroplast, which generally produces an elliptically polarised transmitted beam. This is similar to the action of a birefringent particle, and this effect is termed *form birefringence* or *shape birefringence* [23]. The small orbital torque is due to the interaction between the elliptical focal spot of the beam and the shape of the chloroplast. The ellipticity of the focal spot results when a plane-polarised beam of circular cross-section is focussed to a diffraction-limited spot [19, 24].

The dependence of the torque on the size and shape of an oblate spheroid is shown in figure 6. Since the difference in polarisability of the spheroid along the long and short axes increases with increasing aspect ratio, the torque increases as the aspect ratio increases. For small particles, the torque increases as the particle size increases, because the optical thickness and therefore the phase shift between the plane-polarised components parallel to the long and short axes, and the particle intercepts more of the beam as its cross-sectional area increases. Once the particle becomes larger than the beam, the illuminated portion of the particle is approximately rotationally symmetric about the beam axis, and the torque becomes smaller with increasing particle size. The largest possible torque is generated when the particle is as large as possible, while retaining maximum rotational asymmetry

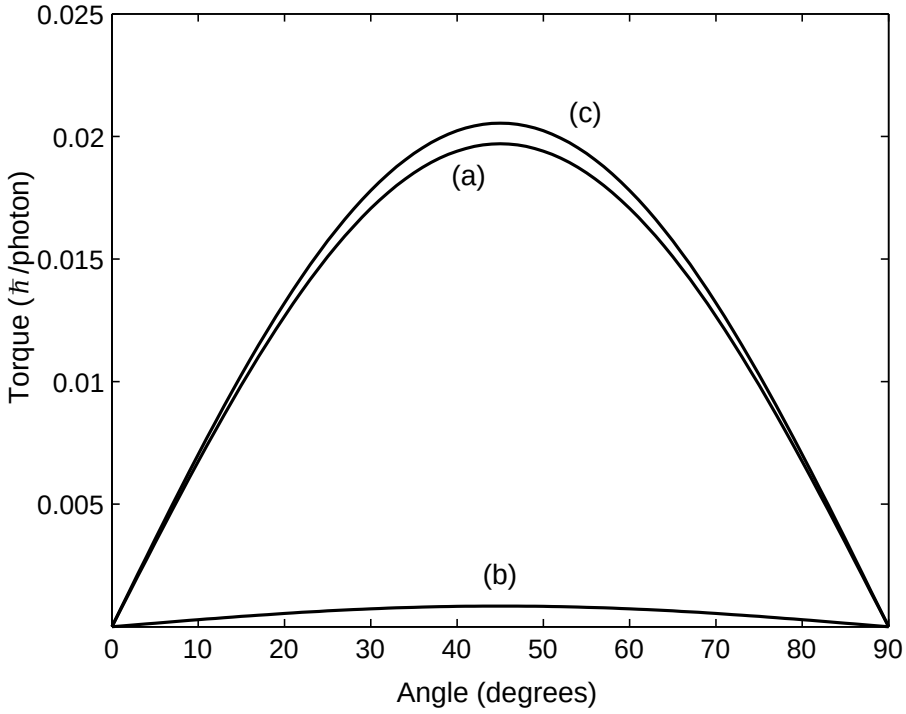

Figure 5: Spin and orbital components of torque. The (a) spin and (b) orbital components of (c) the total torque acting to align a chloroplast with the plane of polarisation of the trapping beam are shown. The chloroplast is already aligned with the beam axis, and the torque is about the beam axis.

of the illuminated portion of the particle. This occurs when the semi-minor axis is approximately equal to the beam waist radius.

Similar alignment effects can be expected for other types of non-spherical particles in optical traps; alignment of short rods has been recently reported [25]. Since the alignment torque due to non-spherical shape is relatively small compared to the torque that can be obtained by using birefringent particles, it might not be observed in all cases; for example, Cheng et al. recently trapped thin PMMA disks, but failed to observe alignment [26].

5 Conclusion

We have demonstrated that the non-spherical shape of chloroplasts is sufficient to allow controllable alignment with optical tweezers using a single plane-polarised Gaussian beam. The chloroplast aligns with one long axis along the beam axis, and the other long axis in the plane of polarisation of the beam. Since the plane of polarisation of the trapping beam can be rotated using a half-wave plate, the orientation of the chloroplast can be controlled. This method of alignment can be applied to other non-spherical objects that have two long axes. Since the diffraction-limited focal spot of a strongly focussed plane polarised beam is slightly elliptical in shape, the focal spot shape might contribute somewhat to the torque. However, our calculations show that the torque is predominantly due to circular polarisation induced in the transmitted beam by the shape of the chloroplast.

References

[1] Ashkin, A., 1997, *Proceedings of the National Academy of Sciences of the USA*, **94**, 4853-4860.

[2] Friese, M. E. J., Enger, J., Rubinsztein-Dunlop, H. and Heckenberg, N. R., 1996, *Physical Review A*, **54**, 1593–1596.

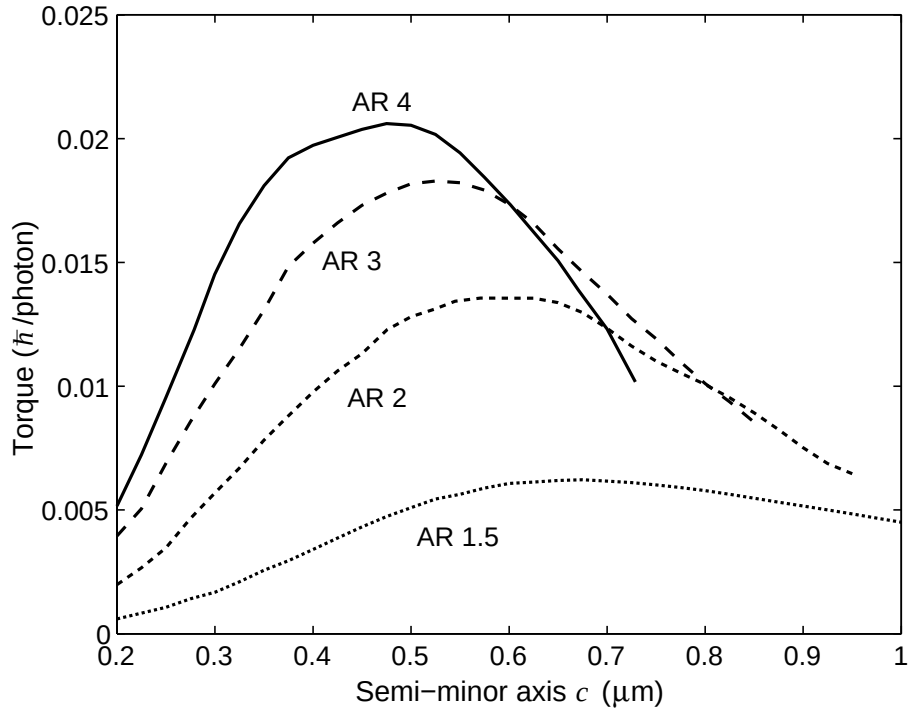

Figure 6: Dependence of torque on aspect ratio. The maximum torque acting to align an oblate spheroid with the plane of polarisation, which occurs when the angle between them is 45°, is shown for spheroids with aspect ratios of 1.5, 2, 3, and 4.

[3] Friese, M. E. J., Nieminen, T. A., Heckenberg, N. R., and Rubinsztein-Dunlop, H., 1998 *Optics Letters*, **23**, 1–3.

[4] Higurashi, E., Ohguchi, O., Tamamura, T., Ukita, H., and Sawada, R., 1997, *Journal of Applied Physics*, **82**, 2773–2779.

[5] Friese, M. E. J., Nieminen, T. A., Heckenberg, N. R., and Rubinsztein-Dunlop, H., 1998 *Nature*, **394**, 348–350. (Erratum, 1998, *Nature*, **395**, 621.)

[6] Galajda, P., and Ormos, P., 2002, *Journal of Optics B*, **4**, S78-S81.

[7] Paterson, L., MacDonald, M. P., Arlt, J., Sibbett, W., Bryant, P. E., and Dholakia, K., 2001, *Science*, **292**, 912–914.

[8] O'Neil, A. T., and Padgett, M. J., 2002, *Optics Letters*, **27**, 743–745.

[9] Santamato, E., Sasso, A., Piccirillo, B., and Vella, A., 2002, *Optics Express*, **10**, 871–878.

[10] Ashkin, A., Dziedzic, J. M., and Yamane, T., 1987, *Nature*, **330**, 769–771.

[11] Nieminen, T. A., Rubinsztein-Dunlop, H., and Heckenberg, N. R., 2001, *Journal of Quantitative Spectroscopy and Radiative Transfer*, **70**, 627–637.

[12] Mishchenko, M. I., Hovenier, J. W., and Travis, L. D. (editors), 2000, *Light scattering by nonspherical particles: theory, measurements, and applications* (San Diego: Academic Press).

[13] Waterman, P. C., 1971, *Physical Review D*, **3**, 825–839.

[14] Mishchenko, M. I., 1991, *Journal of the Optical Society of America A*, **8**, 871–882.

[15] Nieminen, T. A., Rubinsztein-Dunlop, H., Heckenberg, N. R., and Bishop, A. I., 2001, *Computer Physics Communications*, **142**, 468-471.

[16] Ren, K. F., Gréhan, G., and Gouesbet, G., 1996, *Applied Optics* **35**, 2702–2710.

[17] Jackson, J. D., 1999, *Classical electrodynamics* (New York: John Wiley), pp.425–439.

[18] Nieminen, T. A., Rubinsztein-Dunlop, H., and Heckenberg, N. R., 2003, *Journal of Quantitative Spectroscopy and Radiative Transfer*, **79–80**, 1019–1029.

[19] Nieminen, T. A., Rubinsztein-Dunlop, H., and Heckenberg, N. R., 2003, *Journal of Quantitative Spectroscopy and Radiative Transfer*, **79–80**, 1005–1017.

[20] Crichton, J. H., and Marston, P. L., 2000, *Electronic Journal of Differential Equations*, **Conference 04**, 37–50.

[21] Bayoudh, S.,Mehta, M., Rubinsztein-Dunlop, H.,Heckenberg, N. R., and Critchley, C., 2001, *Journal of Microscopy*, **203**, 214–222.

[22] Jones, R. C., 1945, *Physical Review*, **68**, 93–96.

[23] Born, M. and Wolf, E., *Principles of Optics* (Cambridge: Cambridge University Press), pp.705–708.

[24] Sales, T. R. M., 1998, *Physical Review Letters*, **81**, 3844–3847.

[25] Bonin, K. D., Kourmanov, B., and Walker, T. G., 2002, *Optics Express*, **10**, 984–989.

[26] Cheng, Z., Chaikin, P.M., and Mason, T.G., 2002, *Physical Review Letters*, **89**, 108303.

Acknowledgements

Part of this work was supported by The University of Queensland and the Australian Research Council.